

NASA Technical Memorandum 103641

Surface Settling in Partially Filled Containers Upon Step Reduction in Gravity

Mark M. Weislogel and Howard D. Ross
Lewis Research Center
Cleveland, Ohio

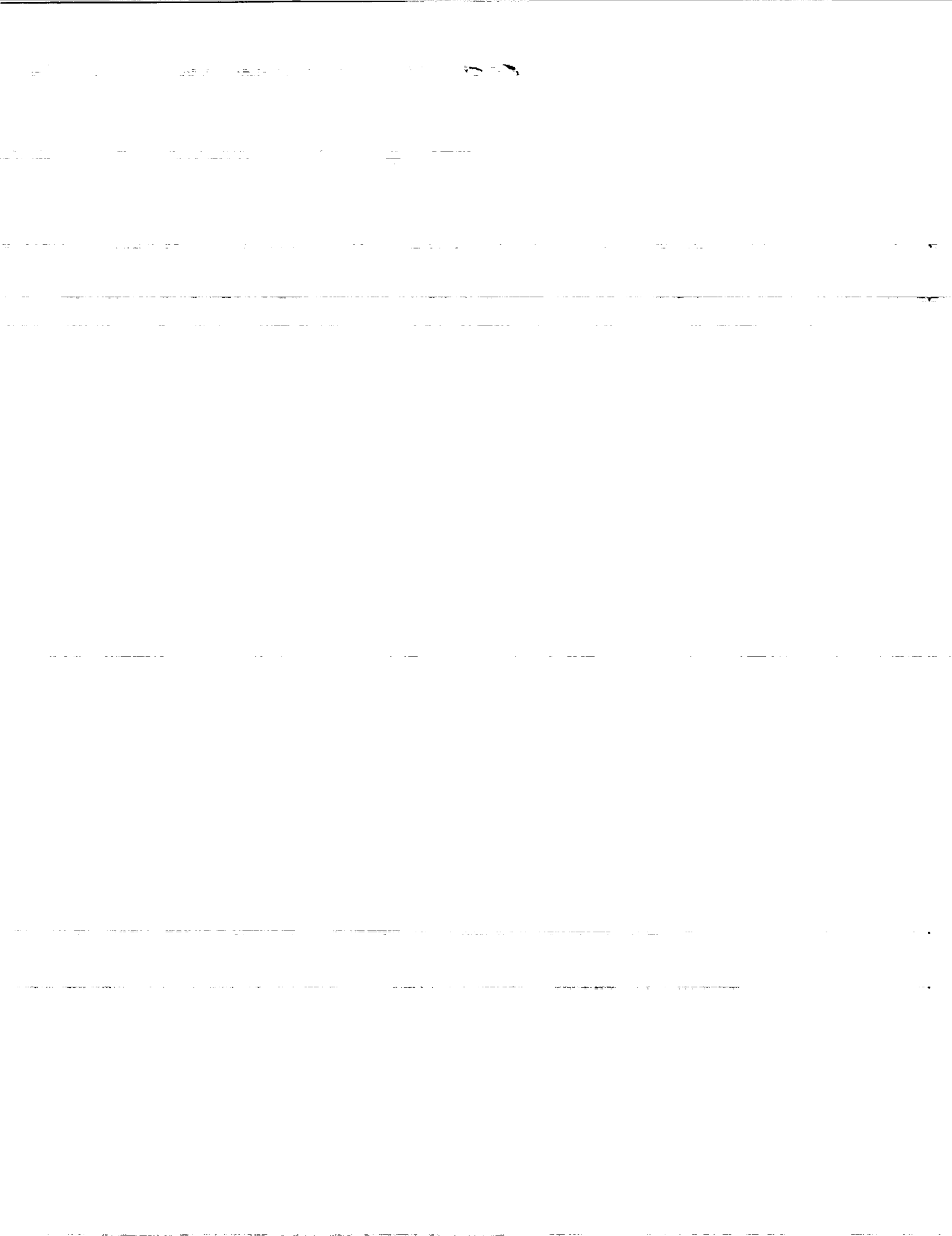
November 1990

(NASA-TM-103641) SURFACE SETTLING IN
PARTIALLY FILLED CONTAINERS UPON STEP
REDUCTION IN GRAVITY (NASA) 19 p CSCL 20D

N91-14556

Unclas
G3/34 0317626

NASA



Surface Settling in Partially Filled Containers upon Step Reduction in Gravity

Mark M. Weislogel
Howard D. Ross

National Aeronautics and Space Administration
Lewis Research Center
Cleveland, Ohio 44135

Summary

A large literature exists concerning the equilibrium configurations of free liquid/gas surfaces in reduced gravity environments. Such conditions generally yield surfaces of constant curvature meeting the container wall at a particular (contact) angle. The time required to reach and stabilize about this configuration is less studied for the case of sudden changes in gravity level, e.g. from normal- to low-gravity, as can occur in many drop tower experiments. The particular interest here was to determine the total reorientation time for such surfaces in cylinders (mainly), as a function primarily of contact angle and kinematic viscosity, in order to aid in the development of drop tower experiment design. A large parametric range of tests were performed and, based on an accompanying scale analysis, the complete data set was correlated. The results of other investigations are included for comparison.

1. Motivation and Background

The use of drop towers to study liquid behavior in low gravity environments is common. Due to the step reduction in gravity level, a characteristic of most towers, reorientation of free liquid surfaces often occurs upon entry into low gravity. For cylinders, the degree of reorientation is dependent on the contact angle (θ) of the particular liquid/solid pair and the change in system

Bond number (Bo), where

$$Bo = \frac{\rho a R^2}{\sigma} \quad (1)$$

with ρ , a , R , and σ denoting liquid density, acceleration due to gravity or other force, cylinder radius, and fluid interfacial tension, respectively.

In general, the Bond number of equation (1) is a ratio of body forces to capillary forces and can change several orders of magnitude during the drop release process. In cases where the forces influencing free liquid interface shapes shift from the gravity dominated case ($Bo \gg 1$) to the situation where capillary forces dominate ($Bo \ll 1$), surface reorientation is most pronounced upon entry into low gravity; the fluid will flow from a "flat" configuration towards its low gravity equilibrium shape, one generally of constant curvature meeting the container wall at the contact angle of the system as pictured in Figure 1. Dependent on the damping of the system, an overshoot can result and oscillation about the equilibrium surface shape occurs until damped. In many cases the normal and low gravity equilibrium surface configurations are determinable [1]. However, the transients associated with the reorientation have not as of yet been quantified.

A number of related analyses have been performed concerning surface reorientation and/or oscillation in low gravity environments [2-13]. A main thrust of these studies has focused on externally forced systems and the problem of lateral

sloshing. In addition, fluids and tank geometries were selected which allowed legitimate inviscid flow approximations with a nearly 0° contact angle condition at the wall. Most specifically, references [9] and [12] approach the objectives of this study. Unfortunately, the former used low viscosity fluids and did not have ample low gravity time to determine a total settling time. The latter used a similar experimental approach as that of this study, but to observe a distinctly unrelated phenomenon. In a small set of preliminary experiments Ross and Pline [13] studied axial oscillations and determined qualitatively that surface oscillations and damping were strong functions of viscosity and contact angle. This effort expands the data base of these earlier studies, quantifies the settling times for a number of liquid/container (with air) systems, and presents functional relationships based on a scale analysis to determine the general settling times for other cylindrical systems.

2. Scale Analysis

A scale analysis was performed to identify the important parameters for which the surface settling time data of this study could be presented. The general form of the scaled parametric equations was then used for correlation purposes.

The notation and language of this section follow those of Bejan [14], where commas between parameters denote some functional relationship, normally addition, while the similar sign (\sim) denotes "of general order". Actual operators ($\times, +, \dots$) are retained only when known. Dividing by scaled quantities often demands physical insight into the problem since, for example, the scale function $1/(\alpha^2, 1)$ could also be interpreted as $(\alpha^{-2}, 1)$. Scale constants appearing in equations are considered $O(1)$ unless they arise from some known relationship.

2.1 Scaled Momentum Equation.

The analysis begins with the momentum equation written in cylindrical coordinates for the axial component, z ,

$$\frac{\partial V_z}{\partial t} + V_r \frac{\partial V_z}{\partial r} + V_z \frac{\partial V_z}{\partial z} = -\frac{1}{\rho} \frac{\partial P}{\partial z} +$$

$$\nu \left(\frac{\partial^2 V_z}{\partial r^2} + \frac{1}{r} \frac{\partial V_z}{\partial r} + \frac{\partial^2 V_z}{\partial z^2} \right) + ng \quad (2)$$

where ng represents the body force term, n being the ratio of the low gravity level to normal earth gravity¹. Direct scaling of each term in the above equation follows when an axial length scale is determined. This scale, Z , is selected as the axial displacement of the meniscus between an assumed initially flat interface and a steady end state surface condition of constant curvature ($n = 0$). Figure 1 depicts Z geometrically as a function of the contact angle (θ) and the radius (R) of the cylinder.

A time scale, t_f , for the momentum equation is defined as a "flow time" or characteristic response time for the system. By introducing the scale relations $V_z \sim Z/t_f$ and $-\partial P/\partial z \sim \sigma \cos \theta/RZ$, and by eliminating Z for the geometrically equivalent αR , the momentum equation may be rewritten as the scale equation

$$\frac{\alpha R}{t_f^2} \sim \frac{\sigma \cos \theta}{\rho \alpha R^2}, \frac{\nu}{\alpha t_f R} (\alpha^2, 1), ng \quad (3)$$

where

$$\alpha = \frac{1 - \sin \theta}{\cos \theta} \quad (4)$$

and ranges $0 \leq |\alpha| \leq 1$. Grouping the time-dependent terms of equation (3), the requirement for which ng may be ignored is the case of $Bo_n \ll 1$, or

$$Bo_n = \frac{\rho ng R^2}{\sigma (1 + \sin \theta)} \ll 1 \quad (5)$$

where Bo_n is a contact angle-dependent, low gravity Bond number. This condition is satisfied for all of the tests performed in this study and for a great many other drop tower experiments due to a general size limitation. As a result, the body force term need not be considered

¹Neglecting the body force term, as will be accomplished shortly, produces similar scale results as would the analysis if it had begun with the momentum equation for the radial component. Axisymmetric reorientation of the fluid is assumed, or $V = V(r, z, t)$. Also, when limited to the liquid/gas interface scenario, the momentum balance for the gaseous phase may be ignored.

in the scale analysis except to determine the initial condition of the surface. Thus, the scaled terms of importance are the unsteady, capillary, and viscous terms, or

$$\frac{\alpha R}{t_f^2}, \frac{\sigma \cos \theta}{\rho R^2 \alpha}, \frac{\nu}{t_f R \alpha} (1, \alpha^2) \quad (6)$$

respectively. The time scale, t_f , may then be determined for the particular cases as listed below:

unsteady ~ capillary; when $\zeta(1, \alpha^2) \ll 1$

$$t_{f_1} \sim \frac{R^2}{\nu} \zeta \alpha^2 \quad (7)$$

capillary ~ viscous; when $\zeta^2(1, \alpha^2)^2 \gg 1$

$$t_{f_2} \sim \frac{R^2}{\nu} \zeta^2 \alpha^2 (1, \alpha^2) \quad (8)$$

unsteady ~ viscous; when $\zeta(1, \alpha^2) \gg 1$

$$t_{f_3} \sim \frac{R^2}{\nu} \frac{\alpha^2}{(1, \alpha^2)} \quad (9)$$

where

$$\zeta = \nu \left(\frac{\rho}{R \sigma \alpha^2 \cos \theta} \right)^{1/2} \quad (10)$$

When the condition of $\zeta \gg 1$ is met, the expressions of equations (8) and (9) are valid for t_f . Therefore,

$$t_{f_2}, t_{f_3} \sim \frac{R^2}{\nu} \zeta^2 \alpha^2 (1, \alpha^2), \frac{R^2}{\nu} \frac{\alpha^2}{(1, \alpha^2)} \quad (11)$$

or

$$t_{f_2}, t_{f_3} \sim \frac{R^2}{\nu} \frac{\alpha^2}{(1, \alpha^2)} [\zeta^2(1, \alpha^2), 1] \quad (12)$$

Since $\zeta \gg 1$, $\zeta^2 \gg 1$ and the contribution of t_{f_3} in equation (12) is negligible, and subsequently ignored. This leaves only t_{f_1} and t_{f_2} for consideration.

The general forms of equations (7) and (8) are well known [15]. The uniqueness of these results, however, is the inclusion of contact angle effects

associated with "nearby" walls, which, by significantly altering the shape of the surface, can also greatly influence the dynamic behavior of the fluid.

2.2 Scaled Energy Equation.

The desired settling time scale, t_s , will be some function of t_f . To determine this relationship, a general end state energy balance may be written

$$\Delta E_g + \Delta E_\sigma = E_\mu \quad (13)$$

where subscripts g and σ denote the change in hydrostatic and interfacial potential energies respectively. E_μ represents the viscous dissipation by which the potential energy is converted to heat. Accurate theoretical values for the two left hand quantities may be determined. However, E_μ is inherently a scaled term in this analysis, therefore, each term is presented in a generalized scale form:

$$\Delta E_g \sim \frac{\pi}{2} k (\beta \rho g R)^2 H^3 f_p, \frac{\pi}{2} \rho g R^2 H^2 \quad (14)$$

$$\Delta E_\sigma \sim 2\pi R^2 f_1 \sigma \cos \theta \quad (15)$$

$$E_\mu = \mu \int_{t_s} \int_V \Phi dV dt \sim \frac{\pi \mu R^3}{\alpha^2} f_2 f_\alpha \int_0^{t_s} \frac{1}{t_f^2} dt \quad (16)$$

where

$$f_p = \bar{p}^2 + \bar{p} + \frac{1}{3} \quad (17)$$

$$f_1 = \frac{\alpha}{\cos^2 \theta} - \alpha^2 \left(\frac{2 + \sin \theta}{3 \cos \theta} \right) - \frac{A_i}{2\pi R^2 \cos \theta} \quad (18)$$

$$f_2 = \alpha - \frac{\alpha^2}{3} \left(\frac{2 + \sin \theta}{\cos \theta} \right) \quad (19)$$

k , β , and \bar{p} represent the fluid elasticity (units of pressure), compressibility coefficient ($\nu^{-1} \partial \nu / \partial P$), and dimensionless reference pressure, $P_o / \rho g H$, respectively [16], with P_o being the ambient pressure of the gas phase. H is the height of the liquid column and the volume of the fluid is denoted by V . The functions f_1 and f_2 result from geometric considerations. Specifically, f_1

arises from the known change in interfacial area² and f_2 from the volume of fluid involved in the re-orientation. A_i is the initial liquid/gas interfacial area and is a function of θ and the initial, normal gravity Bond number ($Bo_i = \rho g R^2 / \sigma$). f_α is a collection of the scaled nonlinear terms of the dissipation function (Φ) and may be expressed as

$$f_\alpha \sim (1, \alpha^2, \alpha^4) \quad (20)$$

ΔE_g contains energies associated with fluid compressibility and the initial normal gravity pressure gradient of the standing liquid column. The former may be neglected since the fluids of this experiment are virtually incompressible ($\beta \rightarrow 0$). Comparing the relative importance of ΔE_g (with $\beta = 0$) to ΔE_σ , the Bond number, Bo_H , based on liquid column height is defined as

$$Bo_H = \frac{\Delta E_g}{\Delta E_\sigma} = \frac{\rho g H^2}{f_1 \sigma \cos \theta} \quad (21)$$

For all cylinders we studied, $Bo_H \gg 1$, implying $\Delta E_g \sim \Delta E_\sigma$. However, the experimentally observed settling time was independent of H . Subsequent flow visualization via particle seeding and a laser light sheet revealed that the fluid motion was limited to the near-surface region contained within the height Z . These two observations suggest that the potential energy stored as gravitational potential (ΔE_g) is not dissipated by viscosity, but by some other mechanism³. Subsequently we remove ΔE_g from the scale equation (13) which yields

$$\Delta E_\sigma \sim E_\mu \quad (22)$$

$$2\pi R^2 f_1 \sigma \cos \theta \sim \frac{\pi \mu R^3}{\alpha^2} f_2 f_\alpha \int_0^{t_s} \frac{1}{t_f^2} dt \quad (23)$$

2.3 Settling Time Scale, t_s .

Substituting the flow time scales of equations (7) and (8) into (23) separately, and noting

²This area includes all phases, both wetted and non-wetted surfaces.

³This explanation is in direct contradiction to that of ref. [12].

$\int_0^{t_s} dt = t_s$, two scaled settling time relations may be expressed with the provided constraints

$$t_{s1} \sim \frac{R^2 f_1 \alpha^4}{\nu f_2 f_\alpha}; \quad \zeta(1, \alpha^2) \ll 1 \quad (24)$$

$$t_{s2} \sim \frac{R^2 f_1 \alpha^4}{\nu f_2 f_\alpha} \zeta^2(1, \alpha^2)^2; \quad \zeta^2(1, \alpha^2)^2 \gg 1 \quad (25)$$

The constraints on equation (24) and (25) allow for the superposition of time scales t_{s1} and t_{s2} leaving

$$t_s \sim t_{s1}, t_{s2} \\ = \frac{R^2 f_1 \alpha^4}{\nu f_2 f_\alpha} (1, \alpha^2)^2 [\zeta^2, (1, \alpha^2)^{-2}] \quad (26)$$

When $Bo_i \gg 1$, implying an initially flat liquid/gas interface ($A_i = \pi R^2$), the quantity f_1/f_2 reduces to a constant $O(1)$. This final assumption noted, equation (26) reduces to

$$t_s \sim \frac{R^2 \alpha^4}{\nu f_\alpha} (1, \alpha^2)^2 [\zeta^2, (1, \alpha^2)^{-2}] \quad (27)$$

which may be more clearly presented as

$$t_s \sim \frac{R^2}{\nu} f(\theta)^{-1} [\zeta^2, g(\theta)] \quad (28)$$

or nondimensionally as

$$\tau = \frac{t_s \nu}{R^2} f(\theta) \sim f(\zeta), g(\theta) \quad (29)$$

This suggests that of the five variables of the problem established ($R, \nu, \rho, \sigma, \theta$), only two parameters, ζ and θ , need be varied experimentally to provide ample data to correlate τ . This is accomplished primarily by varying the fluid viscosity and contact angle in the experiments to be discussed shortly⁴.

⁴The important dimensionless groups may be identified in their more common form by dividing eq. (27) by t_s , multiplying through by R^2/ν , and disregarding contact angle dependence, yielding

$$1 \sim \frac{R\nu\rho}{\sigma t_s}, \frac{R^2}{\nu t_s}$$

Introducing the scale relation $V \sim R/t_s$, and substituting into the above yields

$$1 \sim \frac{\mu V}{\sigma}, \frac{VR}{\nu} \sim Ca, Re$$

where Ca and Re are Capillary and Reynolds number equivalents. This dimensionless number dependence is anticipated [17].

The complexities of $f(\theta)$ and $g(\theta)$ in equation (29) need to be addressed with insight gathered from experiment, since, for example, the scale form of $f(\theta)$

$$f(\theta) \sim \frac{f_\alpha}{\alpha^4(1, \alpha^2)} = \frac{(1, \alpha^2, \alpha^4)}{\alpha^4(1, \alpha^2)^2} \quad (30)$$

may have numerous interpretations.

3. Experiment

3.1 Apparatus.

A schematic of the experimental apparatus is shown in Figure 2. The main components are a circular cylinder whose axis is oriented with the gravity vector, a leveling pad, top and back lighting, and a motion picture camera. The cylinder diameter used for the bulk of the testing was 19.05mm to ensure complete settling within the drop time (less than 2.2 seconds).

The cylinders were drilled out of a rectangular bar of acrylic plastic to minimize refraction associated with the vessel curvature and the mismatched fluid/acrylic refractive indices. All plastic surfaces were polished to optical clarity with progressively finer grit SiC paper and a buffing compound.

For most tests the internal surfaces of the cylinders were prepared by washing them twice in refrigerant-12. They were then rinsed twice with ethanol and cleaned ultrasonically in a warm mild detergent for 30 minutes. After the cleaning, the cylinders were again rinsed with ethanol and allowed to air dry. In this way the surface conditions of the vessels and resultant data were made repeatable.

Poorly leveled cylinders produced lateral sloshing modes easily observed on the films. To reduce this effect a leveling pad was employed. The pad, made of 1cm foam sheet, was squeezed between the cylinder base plate and package floor. Suspended from a wire, the entire experimental apparatus was balanced and the cylinder righted via iterative adjustment of the wingnut fasteners.

Another cause of slosh/swirl during the experiments was attributed to an asymmetric pre-wetting of the cylinder walls which occurred if the fluid was disturbed (sloshed) before the release of the package in the tower. A simple fill

tube/syringe technique was adopted to reduce this effect as is shown in Figure 2. Just prior to the drop a prescribed amount of fluid was injected and the syringe was removed. The lights and camera were initiated approximately 1.5 seconds before the drop. The release of the package began a delay/relay operation which maintained power to the lights and camera during the drop.

3.2 Fluids Selection and Experiments.

The 200 Fluid series (varying viscosity silicone oils) produced by the Dow Corning Corporation and aqueous glycerine solutions allowed variation of the dynamic viscosity without significant variation in other relevant fluid properties. In order to vary only the contact angle with the silicone oils retained as test fluids, a thin film of surface modifier (F-723 supplied by the 3M Co.) was applied to the cylinder walls. The film was applied just prior to each drop and just after each cleaning procedure by filling the cylinder with the surface modifier as a liquid and slowly draining it from the bottom. Two coats of F-723 were applied to each cylinder for these tests and the "coated" cylinder was allowed to air dry. The relevant properties for the silicone oils and other fluids are listed in Table 1. As seen from the table three decades of ζ (with $\theta = 0^\circ$) were obtained by use of 0.65 through 200.0cSt oil.

A series of tests was also performed using aqueous ethanol mixtures in un-coated cylinders. Since distilled water and ethanol produce equilibrium contact angles of 80° and 0° on acrylic, respectively, combinations of the two fluids were selected to produce a range of angles. The surface tensions, viscosities, and densities of these solutions and those of the aqueous glycerine solutions were measured specifically for this research work using standard laboratory procedures and are shown in Table 1 with their respective uncertainties. The equilibrium contact angles for each fluid/solid pair were measured using a number of techniques: the capillary tube, a modified Wilhelmy technique, and a sessile drop (tilt-slide) method. Because contact angle hysteresis is a problem for each of these methods, an equilibrium contact angle was determined by a fourth technique exploiting the steady, end state config-

uration of the low-g liquid surface as suggested in [18]. Since the surface forms a shape of constant curvature, a geometric relationship was derived relating the axial length scale, Z , to the contact angle (ref. Fig. 1),

$$\alpha = \frac{Z}{R} = \frac{1 - \sin \theta}{\cos \theta} \quad (31)$$

The contact angle may then be expressed as

$$\theta = \sin^{-1} \left(\frac{1 - \alpha^2}{1 + \alpha^2} \right) \quad (32)$$

where α is determined experimentally. Equilibrium contact angles determined in this manner are listed in Table 2. In each case the equilibrium angles were found to be within the range of hysteresis determined by the above mentioned techniques.

Supplementary tests were performed to note geometric effects and the dynamic behavior of the contact line during the reorientation and settling of the surface. Concerning the former, square vessels were employed for these tests, and, due to their larger characteristic length, the 5 second drop facility at NASA Lewis Research Center was used. Fluid selection was made similarly as with the cylinders in order to vary primarily the fluid viscosity and contact angle. As is the case for capillary flow in corners, stable surfaces result when the condition $\theta > 90^\circ - \psi$ is satisfied [19], where ψ is the half-angle of the corner in question. For the Square vessel $\psi = 45^\circ$ and contact angles in this range were tested. As a point in verification of this criteria, contact angle values which did not satisfy this criteria produced surfaces which, after having "climbed" or wicked up the corners, formed relatively complex shapes or wrapped entirely around the ullage. Unfortunately, the results of these tests were predominantly qualitative as positive identification of the interface was always in question due to a lighting and photographic limitation. It can be said, however, that the general settling behavior for the vessel with square cross section followed similarly that of the right circular cylinder.

The transients of the settling process could not be observed at the contact line for the majority of the tests. This was attributable to

the significantly mismatched refractive indices of the test fluids ($n \doteq 1.35$) and acrylic containers ($n = 1.49$) employed. In order to view the contact line region, a special fluid solution was prepared possessing an identical index of refraction as that of the acrylic. The solution consisted of Cargille Laser Fluid ($n = 1.5$) and 2cSt silicone oil ($n = 1.39$) and was iteratively mixed and measured using a standard refractometer until it matched the value of the acrylic. The precision of the measurement under controlled temperature conditions was better than 0.5%. The viscosity, density, surface tension, and contact angle on an FC-723 coated surface were also measured for the mixture and found to be 14.9cSt, 880kg/m³, 26.3N/m, and 70°, respectively. The dependence of the solution refractive index on temperature was also determined and, for the range of temperatures at which the drop tests were performed, was shown to not produce significant changes in the value.

4. Results and Discussion

4.1 Primitive Variable Dependencies.

Selected surface settling time histories of the meniscus apex for a given cylinder diameter are plotted in Figures 3 and 4 for the silicone oil tests. Figure 3 is presented to display viscous effects ($\theta = \text{constant}$) while Figure 4 is to show contact angle effects ($\nu = \text{constant}$). The data for these figures were obtained from the film records by taking measurements, for the most part, every 1/64 sec to $\pm 0.05\text{mm}$. Data read at 1/128 sec produced identical results. Settling time and frequency characteristics were directly obtained from such data and are compiled in Table 2 for the various tests performed.

The frequencies of the surface oscillations were found to be regularly periodic and were determined by averaging peak-to-peak values—the number of peaks (nodes) used in the averages are listed in Table 2. The settling time was defined as the point at which regular oscillations were no longer detectable or, in the case of the high viscosity fluids experiencing creep, the point at which the axial meniscus location became steady in time. In some cases these settling characteristics were additive. This is exemplified in Figure

3 for the 10.0cSt silicone oil test. The settling time for such a case was defined as 1.75sec and not 0.75sec.

Due to the high magnification of the camera on the cylinder, the fore-field of view (leading edge of the meniscus) was blurred yielding a "thick" initial interface ($\sim 0.3mm$) which was difficult to identify consistently. As a result, the initial surface position varied to the extent that the equilibrium surface location did not always coincide for identical contact angles (refer Figure 3). However, frequency and settling time measurements were not affected by this condition.

The dynamics at the contact line during the process are illustrated in Figure 5 for the index-matched solution. It is evident from the figure that oscillation at the contact line is not present. It should be stated, however, that due to the refractive index limitation, fluid viscosities below $zcSt$ could not be tested and non-oscillatory behavior of the contact line, or even contact angle, should not be assumed for all values of ζ . For the case of Figure 5, variance in the contact angle could not be determined.

The raw frequency and settling time data for the silicone oil tests is presented in Figures 6 and 7 for a cylinder of radius 9.52mm. The damping ratio with $\theta = 0^\circ$, or $\zeta_{\theta=0^\circ} = \nu(\rho/R\sigma)^{1/2}$, is used on the abscissa of both figures. This is done to display the effects of varying contact angle on the resulting settling characteristics. It should be noted that the contact angles for the silicone oil/F-723 tests ranged from 32° to 67° (points left to right on plots in order as listed in Table 2). Regardless of this fact, a strong contact angle effect is noticeable. The settling time data for the silicone oil/F-723 tests suggests an upward trend for large values of ζ as does that of the silicone oil/acrylic system ($\theta = 0^\circ$) at $\zeta \doteq 0.003$.

4.2 Nondimensionalized Experimental Results.

The data of Figure 7 is again displayed on Figure 8 with t_s nondimensionalized and plotted against ζ following the form of equation (29). The function $f(\theta) = 1 + \alpha^2$ is used so that

$$\tau = \frac{t_s \nu}{R^2} (1 + \alpha^2) \quad (33)$$

Also shown on Figure 8 is the aqueous ethanol

data set with $R = 9.52mm$. The primary variable for the aqueous ethanol mixtures was the contact angle which varied from 5° to 67° , the lower values collapsing on the $\theta = 0^\circ$ silicone oil/acrylic curve. From this figure three characteristics of the τ - ζ relationship were noted for the range of ζ tested: 1) for θ held constant, τ obeys a power law dependence on ζ , 2) for constant ζ , τ decreases with increasing θ , and 3) for low ζ (≤ 0.003) τ appears to approach a constant value. This latter observation is suggested in Figure 8 by the silicone/acrylic data and by $g(\theta)$ in equation (29) which is a constant for any given θ . Exploiting these observations an empirical correlation was developed using the relationship

$$\tau \doteq 10^B \zeta^A + g(\theta) = \phi(\zeta, \theta) \quad (34)$$

where

$$\begin{aligned} \tau &= \frac{t_s \nu}{R^2} (1 + \alpha^2) \\ \zeta &= \nu \left(\frac{\rho}{R\sigma\alpha^2 \cos \theta} \right)^{1/2} \\ \alpha &= \frac{1 - \sin \theta}{\cos \theta} \\ A &= -1.2\alpha^2 + 2.2\alpha + 0.28 \quad (35) \\ B &= 3.9A - 3.32 \quad (36) \\ g(\theta) &= 0.01\alpha^2 \quad (37) \end{aligned}$$

A , B , $g(\theta)$, and the function $(1 + \alpha^2)$ in τ were determined empirically in terms of α . Equation (34) solved explicitly for the settling time t_s produces

$$t_s = \frac{R^2}{\nu} (1 + \alpha^2)^{-1} (10^B \zeta^A + 0.01\alpha^2) \quad (38)$$

The correlation of the data when represented empirically by ϕ and τ is illustrated in Figure 9 with the aqueous glycerine series and data from other sources added [12,13]. The data of Kaukler agree well with the correlated data of this study as do those of Ross and Pline. Both researchers used different-sized cylinders, the latter with a radius three times that of the majority of this study. Additional data points were obtained in this study using distilled water and methanol in acrylic cylinders with and without F-723. These are also included on the plot.

The correlated settling time of equation (38) for surface reorientation in right circular cylinders upon release in a drop tower permits explicit calculation to within a factor of two for the entire range of parameters tested; namely, $0.65 \leq \nu \leq 500(cSt)$, $9.52 \leq R \leq 30(mm)$, $760 \leq \rho \leq 1238(kg/m^3)$, $0.0159 \leq \sigma \leq 0.0695(N/m)$, and $0^\circ \leq \theta \leq 70^\circ$. For over 85% of the data the accuracy of equation (38) is better than $\pm 50\%$. For the specific case of $\theta = 0^\circ$ the relation simplifies to

$$t_s = \frac{2R^2}{\nu} (50\zeta^{1.28} + 0.01) \quad (39)$$

and appears accurate to $\pm 20\%$.

4.3 Sources of Scatter.

Sources of scatter include container cleanliness, wall pre-wetting, photographic limitations, and variations in the drop release mechanism which can cause non-axial accelerations. To the extent possible, these effects were minimized by the methods described earlier.

The data correlating least well are the aqueous glycerol mixtures which have large contact angles and σ/ρ values roughly 3 times those of the other fluids tested. For these mixtures, numerous initial surface configurations were observed with only slight changes in fill technique, due to hysteresis effects common to large contact angle systems. As recognized in section 2.2, the normal gravity, initial shape of the liquid surface affects the settling time, t_s , through A_i in equation (18). Hence the observed variability in initial shape likely caused the unsatisfactory correlation.

The low viscosity fluids also produced slightly variable initial surface configurations depending on the disturbances to the cylinders as they were handled just prior to the drop. These fluids were more likely to pre-wet walls and so change the initial surface curvature. However, through care and repeated tests, this problem was virtually eliminated.

4.4 Settling Time Dependence on θ .

The general effect of varying θ on t_s may be seen by plotting t_s of equation (38) against θ . This is presented in Figure 10 using the properties of silicone oil with $R = 9.52mm$. The curves of constant $\nu(\rho/R\sigma)^{1/2}$ ($= \zeta_{\theta=0^\circ}$) demonstrate

the contact angle effects; namely, a maximum time required for surfaces to settle occurs at some intermediate value of θ depending on the damping of the system. The relationship is also represented in Figure 11 where t_s is plotted against $\nu(\rho/R\sigma)^{1/2}$ for cases of constant θ . It is apparent from both figures that in the vicinity of $\theta = 0^\circ$ the settling times increase as θ increases. This is due to the significant reduction in viscous damping at the wall with only marginal changes in interfacial potential energy. The low viscosity, large contact angle fluids ($\theta > 30^\circ$) rapidly established a pinned contact line and oscillations about this line proceeded until damped. For the same fluids with small contact angle, the first oscillation was severe enough to cause liquid to wet the container wall above the final equilibrium position. Viscous damping at the wall was accentuated in these cases due to the increased wall area in contact with the fluid.

It is also apparent that t_s approaches 0 as θ approaches 90° since the low and normal gravity surface shapes are nearly equivalent (flat). However, in these cases viscous damping is also small and wall damping is essentially nonexistent. Should disturbances be present (axial or non-axial depending on release technique, asymmetric pre-wetting, non-level cylinder, etc.) larger-than-expected settling times may result. The cases of $\theta \simeq 90^\circ$ are also singular points for the correlation ($\zeta \rightarrow \infty$) and values in the near vicinity ($\simeq 85^\circ$) may serve as a conservative estimate given the fact that disturbances *will* occur upon release.

5. Concluding Remarks

A correlation to determine the settling time of fluid surfaces in cylinders has been developed for use in the design of drop tower experiments. The result also provides some guidance for rapidly estimating settling times given a general reduction in body force. This could be useful in actual space applications (e.g. when engine thrust is terminated and liquid in propellant tanks/containers rapidly enters a low gravity environment). Although a wide range of viscosities and contact angles were tested and well correlated, some caution should be taken when extrap-

olating the results to systems with large cylinder radii since this parameter was varied only over a factor-of-three range.

References

1. Concus, P.: *Static Menisci in a Vertical Right Circular Cylinder*, J. Fluid Mech. 34, 481-495, 1968
2. Labus, T.L.: *Natural Frequency of Liquids in Annular Cylinders under Low Gravity Conditions*, NASA TN D-5412, 1969
3. Salzman, J.A., Masica, W.J.: *Lateral Sloshing in Cylinders under Low Gravity Conditions*, NASA TN D-5058, 1969
4. Satterlee, H.M., Reynolds, W.C.: *The Dynamics of the Free Liquid Surface in Cylindrical Containers under Strong Capillary and Weak Gravity Conditions*, Dept. M.E. Stanford U., Tech. Report LG-2, Stanford, CA, 1964
5. Concus, P., Crane, G.E., Satterlee, H.M.: *Small Amplitude Lateral Sloshing in a Cylindrical Tank with a Hemispherical Bottom under Low Gravity Conditions*, Rep. LMSC/A852007 (NASA-CR-54700), Lockheed Missiles and Space Co., 1967
6. Hollister, M.P., Satterlee, H.M., Cohan, H.: *Liquid Propellant Behavior During Periods of Varying Accelerations*, Rep. LMSC/A874728 (NASA-CR-92082), Lockheed Missiles and Space Co., 1967
7. Stark, J.A., Bradshaw, R.D., Blatt, M.H.: *Low-G Fluid Behavior Technology Summaries*, Rep. N75-14060 (NASA-17814), General Dynamics, 1974. A good overview of the listed references
8. Masica, W.J., Derdul, J.D., Petrash, D.A.: *Hydrostatic Stability of the Liquid-Vapor Interface in a Low-Acceleration Field*, NASA TN D-2444, 1964
9. Siegert, C.E., Petrash, D.A., Otto, E.W.: *Time Response of Liquid-Vapor Interface after Entering Weightlessness*, NASA TN D-2458, 1964
10. Dodge, F.T.: *Vertical Excitation of Propellant Tanks*, NASA SP-106, Chapter 8, 1966
11. McCarty, J.L., Stephens, D.G.: *Investigation of the Natural Frequencies of Fluids in Spherical and Cylindrical Tanks*, NASA TN D-252, 1960
12. Kaukler, W.F.: *Fluid Oscillation in the Drop Tower*, Metallurgical Transactions, Vol. 19A, Nov. 1988, pp 2625-30
13. Ross, H.R., Pline, A.D.: *Equilibrium Times for Gas-Liquid Systems Exposed to Step Changes in Gravity*, AIChE Ann. Mtg., WA DC, Dec. 1988
14. Bejan, A.: *Convection Heat Transfer*, Wiley-Interscience Publication, 1984, p. 19
15. Reynolds, W.C.: *Hydrodynamic Considerations for the Design of Systems for Very Low Gravity Environments*, Dept. M.E. Stanford U., Tech Report LG-1, Stanford, CA, 1961
16. Lamb, H.: *Hydrodynamics*, Dover Publications, 1945, p. 480
17. Dussan V, E.B.: *On the Spreading of Liquids on Solid Surface Static and Dynamic Contact Lines*, Ann. Rev. Fluid Mech., 1979 11:371-400
18. Chai, A.: *Accurate Measurement of Contact Angles*, AIAA 27th Aerospace Sciences Meeting, Reno, Nevada, Jan. 1989
19. Concus, P., Finn, R.: *Continuous and Discontinuous Disappearance of Capillary Surfaces*, in Variational Methods for Free Surface Interfaces, Springer-Verlag, New York, 1987, pp. 197-204

Table 1. Relevant fluid/interfacial properties.

Liquid	$\nu \pm 1\%$ (cSt)	$\rho \pm 5$ (kg/m ³)	$\sigma \pm 5\%$ (N/m)	ζ^*
Silicone Oil	0.65	760	0.0159	0.00146
"	1.0	816	0.0174	0.00222
"	1.5	851	0.0180	0.00334
"	2.0	872	0.0187	0.00442
"	5.0	913	0.0197	0.0110
"	10.0	935	0.0201	0.0221
"	20.0	949	0.0206	0.0440
"	50.0	960	0.0208	0.110
"	100.0	964	0.0209	0.220
"	200.0	967	0.0210	0.440
"	500.0	970	0.0212	1.096
Eth/H ₂ O 20/80(% vol.)	1.74	958	0.0443	0.00262
" 30/70	2.36	937	0.0364	0.00388
" 40/60	2.64	916	0.0328	0.00452
" 50/50	2.75	896	0.0308	0.00481
" 60/40	2.68	875	0.0295	0.00473
" 70/30	2.47	854	0.0275	0.00446
" 80/20	2.36	833	0.0260	0.00433
" 100/0	1.43	791	0.0227	0.00274
Gly/H ₂ O 4.9/95.1 (% mass)	1.04	1010	0.0655	0.00132
" 32.6/67.4	2.25	1072	0.0695	0.00286
" 54.4/45.6	5.36	1127	0.0675	0.00710
" 64.8/35.2	10.6	1155	0.0680	0.0142
" 72.5/27.8	18.5	1177	0.0692	0.0247
" 82.1/17.9	44.4	1205	0.0680	0.0606
" 92.9/7.1	205.0	1238	0.0670	0.285
Methanol	0.75	800	0.0226	0.00145
Distilled Water	1.08	998	0.065	0.00137
i-C ₃ H ₇ OH at 34°C†	1.91	774	0.0200	0.00336
" at 42°C†	1.15	768	0.0190	0.00207

*, ζ with $\theta = 0^\circ$ and $R = 9.525\text{mm}$ unless otherwise specified

†, Data for Kaulkler [12] with $R = 12.5\text{mm}$

Table 2a. Results of experimentation.

Liquid/Solid with Air	Cyl. Radius (<i>m</i>)	$\theta \pm 2^\circ$ (<i>degrees</i>)	Nodes	$\omega \pm 0.2$ (<i>cyc/sec</i>)	$t_s \pm 10\%$ (<i>sec</i>)
Si. Oil 0.65 <i>cSt</i> / Acrylic	0.00952	0°	3	3.1	1.58
" 1.0	0.00952	0°	3	3.0	1.15
" 1.5	0.00952	0°	3	3.4	0.94
" 2.0	0.00952	0°	3	3.7	1.06
" 5.0	0.00952	0°	4	4.6	1.40
" 10.0	0.00952	0°	3	5.3	1.75
" 20.0	0.00952	0°	1	5.8	2.0
" 50.0	0.00952	0°	-	-	2.5 ⁺
" 100	0.00952	0°	-	-	3.25 ⁺
" 10.0*	0.030	~ 0°	3	0.8	5.10
Si. Oil 0.65 <i>cSt</i> / F-723	0.00952	32°	6	5.7	3.38 ⁺
" 1.0	0.00952	44°	12	6.4	2.75 ⁺
" 1.5	0.00952	46°	8	6.7	1.94
" 2.0	0.00952	51°	6	7.0	1.62
" 5.0	0.00952	59°	9	7.0	1.12
" 10.0	0.00952	60°	4	7.1	0.66
" 20.0	0.00952	66°	4	7.3	0.55
" 50.0	0.00952	67°	-	-	0.33
" 100	0.00952	68°	-	-	0.25
" 200	0.00952	66°	-	-	0.10
" 500	0.00952	65°	-	-	0.28
" 100	0.01904	61°	-	-	1.55
" 200	0.01904	65°	-	-	1.67
" 500	0.01904	74°	-	-	2.5 ⁺
" 10.0*	0.030	57°	6	1.4	4.72

+ , Linearly extrapolated value

* , Data from Ross and Pline [13]

- , No measurable oscillations

Table 2b. Results of experimentation (continued).

Liquid/Solid with air	Cyl. Radius (m)	$\theta \pm 2^\circ$ (degrees)	Nodes	$\omega \pm 0.2$ (cyc/sec)	$t_s \pm 10\%$ (sec)
Eth-H ₂ O 20/80 /Acrylic	0.00952	63°	7	10.8	0.84
" 30/70	0.00952	51°	10	10.0	1.15
" 40/60	0.00952	40°	9	7.8	1.54
" 50/50	0.00952	35°	9	7.8	1.42
" 60/40	0.00952	20°	8	6.4	1.38
" 70/30	0.00952	15°	10	6.1	1.79
" 80/20	0.00952	9°	5	5.5	1.50
" 100/0	0.00952	< 5°	3	4.4	1.06
Gly/H ₂ O 4.9/95.1 /Acrylic	0.00952	62°	18	14.1	1.30
" 32.6/67.4	0.00952	66°	22	13.5	1.87
" 54.4/45.6	0.00952	68°	7	12.4	0.75
" 64.8/35.2	0.00952	68°	8	11.9	0.75
" 72.5/27.8	0.00952	70°	6	11.6	0.58
" 82.1/17.9	0.00952	57°	-	-	0.23
" 92.9/7.1	0.00952	57°	-	-	0.12
" 92.9/7.1	0.01904	57°	-	-	1.50
H ₂ O/Acrylic (Eth. rinse)	0.00952	67°	11	14.4	0.82
" (Gly. rinse)	0.00952	54°	14	14.0	1.12
Methanol/Acrylic	0.00952	0°	7	4.5	1.53
Methanol/F-723	0.00952	50°	17	7.9	2.50 ⁺
i-C ₃ H ₇ OH/Glass (34°C) [#]	0.0125	0°	2	1.79	1.4
" (42°C) [#]	0.0125	0°	2	1.6	1.60

+, Linearly extrapolated

#, Data from Kaukler [12]

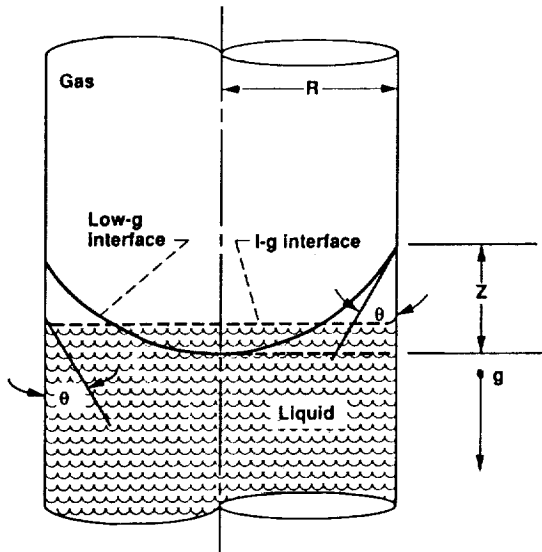


FIGURE 1. - NORMAL AND LOW-GRAVITY INTERFACIAL SURFACES WITH AXIAL LENGTH SCALE Z IN RELATION TO R AND θ .

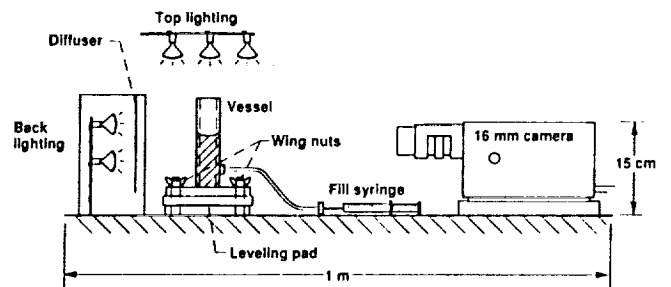


FIGURE 2. - SCHEMATIC OF EXPERIMENTAL APPARATUS.

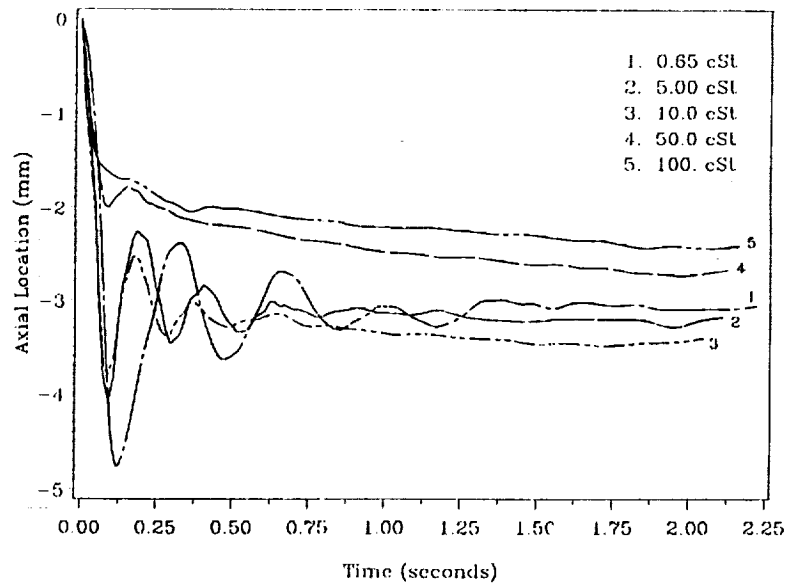


FIGURE 3. - SURFACE SETTLING HISTORIES FOR SILICONE OIL/ACRYLIC PAIR ($\theta = 0^\circ$ AND $R = 9.52$ mm).

ORIGINAL PAGE IS
OF POOR QUALITY

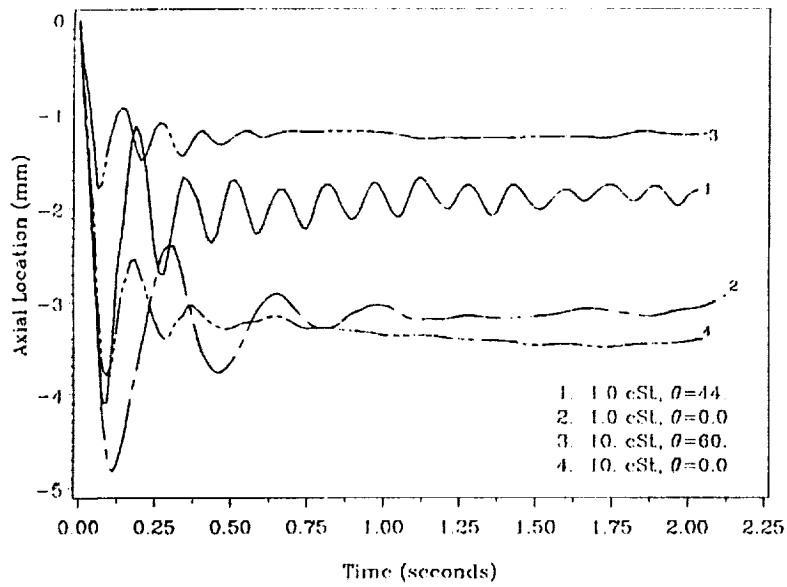


FIGURE 4. - SELECTED SETTLING HISTORIES TO ILLUSTRATE CONTACT ANGLE EFFECTS FOR SILICONE OILS ($R = 9.52$ mm).

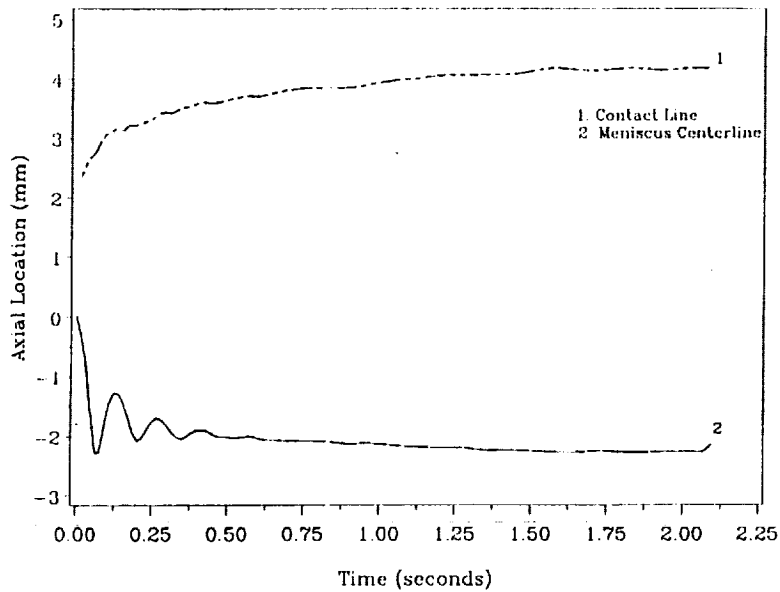


FIGURE 5. - SETTLING HISTORY FOR REFRACTIVE INDEX MATCHED FLUID ($R = 9.52$ mm).

ORIGINAL PAGE IS
 OF POOR QUALITY

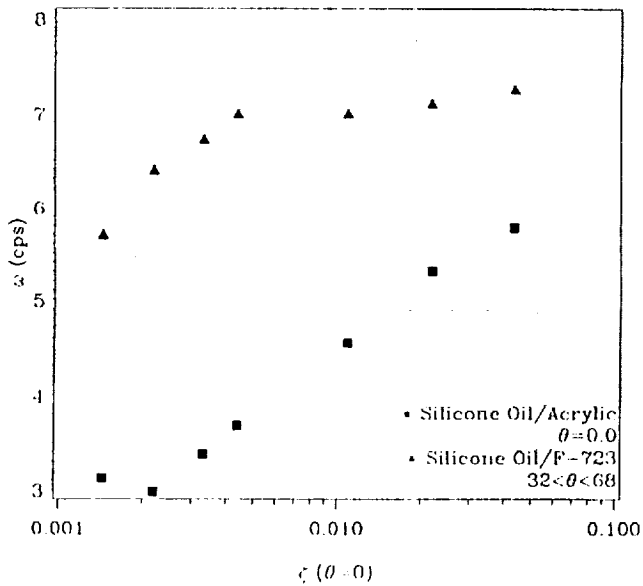


FIGURE 6. - FREQUENCY OF OSCILLATION VERSUS DAMPING RATIO (R = 9.52 mm).

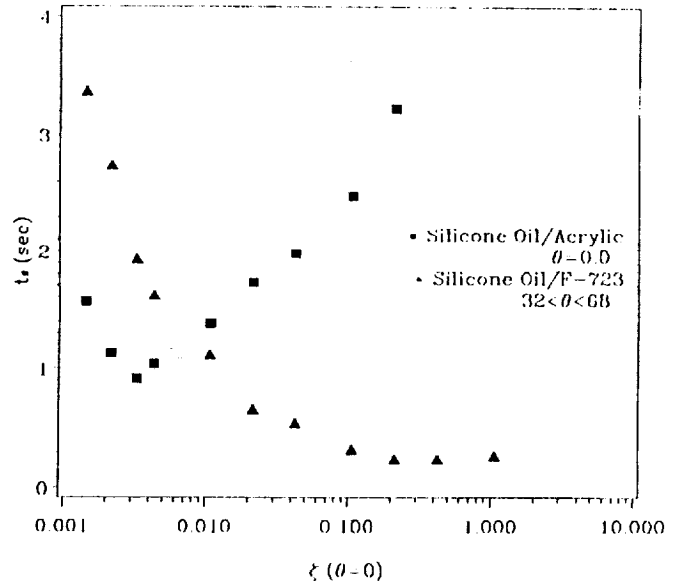


FIGURE 7. - SETTLING TIME VERSUS DAMPING RATIO (R = 9.52 mm).

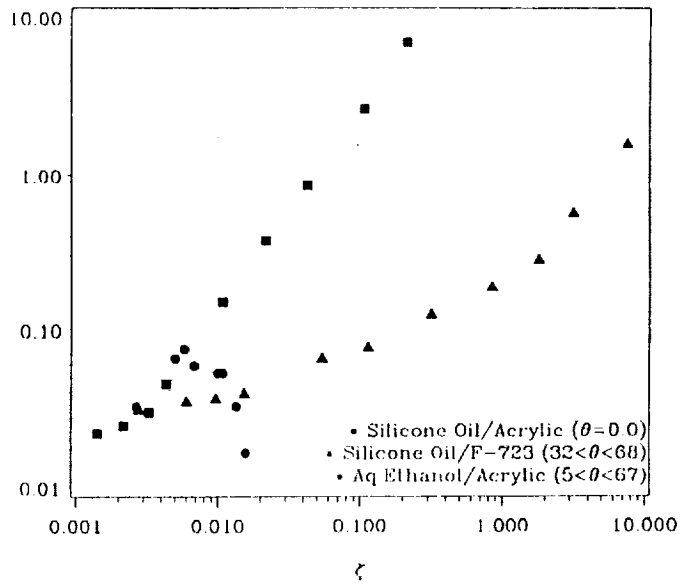


FIGURE 8. - NONDIMENSIONALIZED SETTLING TIME VERSUS DAMPING RATIO (R = 9.52 mm).

ORIGINAL PAGE IS
OF POOR QUALITY

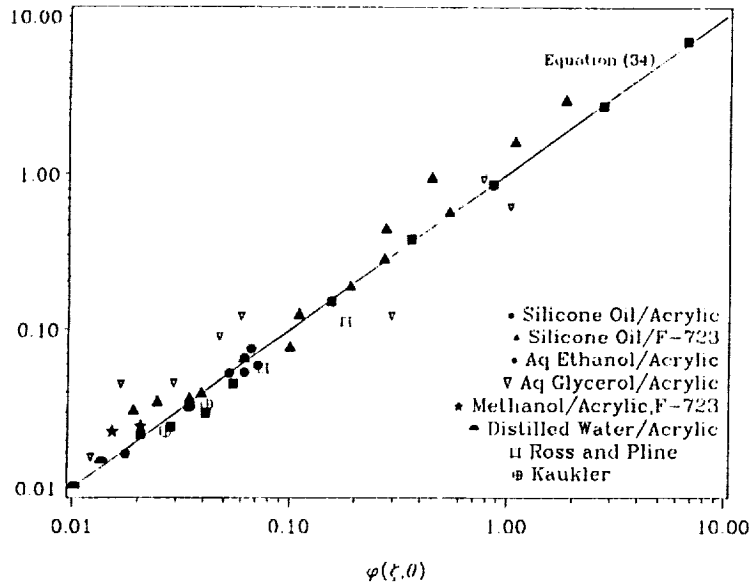


FIGURE 9. - NONDIMENSIONALIZED SETTLING TIME VERSUS CORRELATION FUNCTION $\phi(\xi, \theta)$ FOR ENTIRE DATA SET.

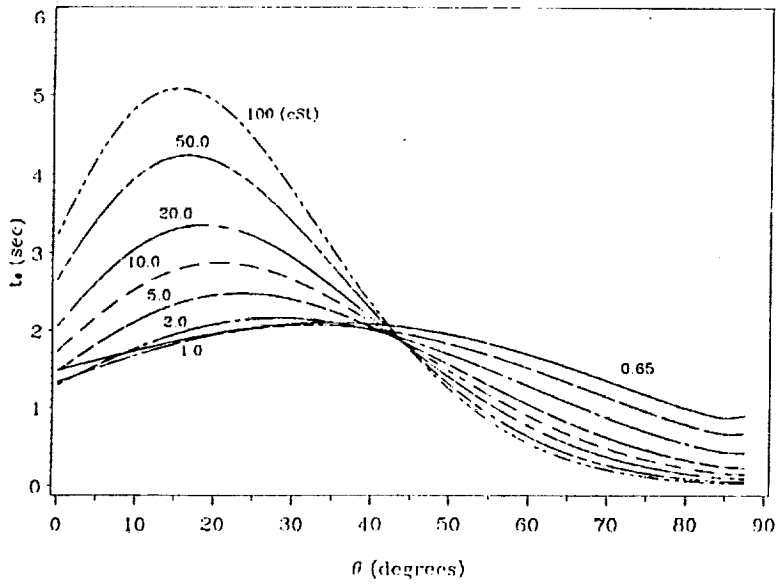


FIGURE 10. - GENERAL DEPENDENCE OF t_s ON θ AS DETERMINED BY EQUATION (38) FOR CASES OF CONSTANT $\nu(\rho/R\sigma)^{1/2}$ (PROPERTIES OF SILICONE OIL FOR THE STATED KINEMATIC VISCOSITY ARE USED WITH $R = 9.52$ mm).

ORIGINAL PAGE IS
OF POOR QUALITY

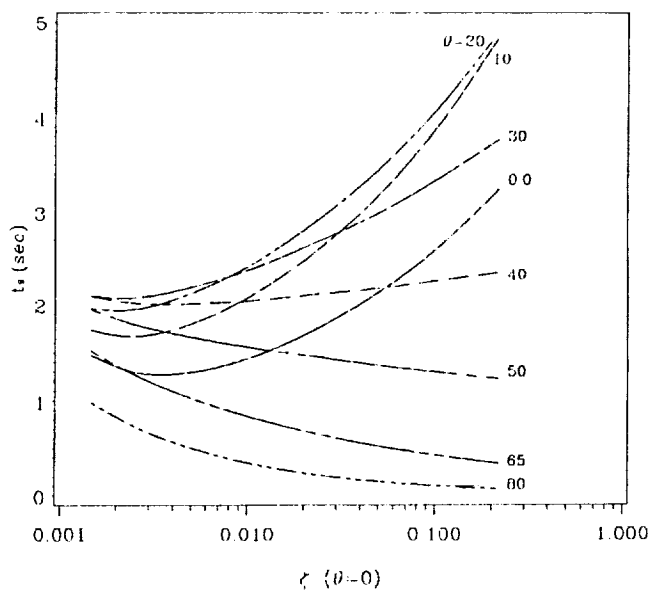


FIGURE 11. - GENERAL DEPENDENCE OF t_s ON $\zeta_{\theta=0}$ AS DETERMINED BY EQUATION (38) (SILICONE OIL, PROPERTIES USED WITH $R = 9.52$ mm).

ORIGINAL PAGE IS
OF POOR QUALITY



Report Documentation Page

1. Report No. NASA TM-103641	2. Government Accession No.	3. Recipient's Catalog No.	
4. Title and Subtitle Surface Settling in Partially Filled Containers Upon Step Reduction in Gravity		5. Report Date November 1990	6. Performing Organization Code
		8. Performing Organization Report No. E-4998	
7. Author(s) Mark M. Weislogel and Howard D. Ross		10. Work Unit No. 674-24-05	11. Contract or Grant No.
		13. Type of Report and Period Covered Technical Memorandum	
9. Performing Organization Name and Address National Aeronautics and Space Administration Lewis Research Center Cleveland, Ohio 44135-3191		14. Sponsoring Agency Code	
		12. Sponsoring Agency Name and Address National Aeronautics and Space Administration Washington, D.C. 20546-0001	
15. Supplementary Notes			
16. Abstract <p>A large literature exists concerning the equilibrium configurations of free liquid/gas surfaces in reduced gravity environments. Such conditions generally yield surfaces of constant curvature meeting the container wall at a particular (contact) angle. The time required to reach and stabilize about this configuration is less studied for the case of sudden changes in gravity level, e.g. from normal- to low-gravity, as can occur in many drop tower experiments. The particular interest here was to determine the total reorientation time for such surfaces in cylinders (mainly), as a function primarily of contact angle and kinematic viscosity, in order to aid in the development of drop tower experiment design. A large parametric range of tests were performed and, based on an accompanying scale analysis, the complete data set was correlated. The results of other investigations are included for comparison.</p>			
17. Key Words (Suggested by Author(s)) Reduced gravity; Contact angle; Surface tension; Interface configuration; Surface reorientation		18. Distribution Statement Unclassified - Unlimited Subject Categories 34 and 88	
19. Security Classif. (of this report) Unclassified	20. Security Classif. (of this page) Unclassified	21. No. of pages 18	22. Price* A03